

# 52/119 GHz Corrugated Horn Design for Earth Observation Applications

J.-P. Adam<sup>1</sup>, Y. Béniguel<sup>1</sup>, A. Berthon<sup>1</sup>, L. Costes<sup>2</sup>, M. Van der Vorst<sup>3</sup>

<sup>1</sup>IEEA, France, jean-pierre.adam@club-internet.fr

<sup>2</sup>EADS Astrium, France, laurent.costes@astrium.eads.net

<sup>3</sup>ESA, The Netherlands, maarten.van.der.vorst@esa.int

**Abstract**— This paper describes the design of a dual frequency corrugated horn. The center operating frequencies are 52.5 GHz and 118.75 GHz. This feed is used to illuminate an offset reflector. Return loss and cross polarization requirements were taken into account. In addition, the far field radiation patterns at both operating frequencies have to overlap.

## I. INTRODUCTION

The presented antenna is a component of an atmospheric sensor. Moreover, it has to be sensible to the oxygen contained in the atmosphere. The figure 1 presents the transmission coefficient of the atmosphere. Two absorption bands are due to the oxygen : around 60 GHz and 120 GHz. These bands are the reason why the center operating frequencies of the presented feed are 52.5 GHz and 118.75 GHz (the operating frequency bands are 50-55 GHz and 110.25-127.25 GHz). In order to test to same point of the atmosphere, the antenna radiation patterns have to be identical at these frequencies. This work is an update of the results presented in [1], with a particular focus on the feed design.

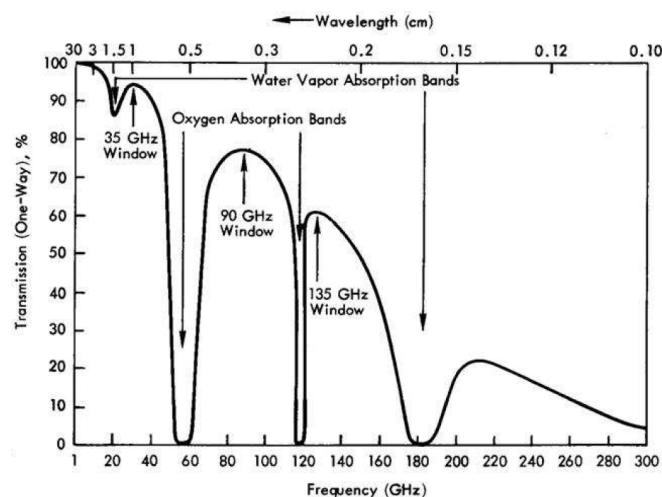


Fig. 1 Atmospheric transmission coefficient for a vertical incidence.

Since the design requirements include a low return loss ( $< -28$  dB) and a low cross polarization ( $< -32$  dB at feed level), a corrugated horn design is considered. According to [2], the

frequencies ratio allows the use of a single depth corrugated horn. Due to the high required beam efficiency of the reflector antenna ( $>95\%$ ), the aperture of the feed is large. In addition, a low flare angle seems necessary to get an acceptable return loss. In other words, the horn is long. In order to study the horn behavior over the whole frequency band in a reasonable CPU time, a shorter horn is considered. This horn has the same throat region, the same output corrugations and the same flare angle as the full horn. It is assumed that the return loss is mostly determined by the throat region. In addition, it is supposed that this shorter horn is long enough to provide a cross polarization level close to the cross polarization level of the full horn.

## II. RETURN LOSS AND CROSS POLARIZATION

### A. Principle

The basic idea of the dual band single depth corrugated horn is that the corrugation depth is close to  $\lambda/4$  at 52.5 GHz and to  $3\lambda/4$  at 118.75 GHz, in order to support the dominant hybrid mode and to get a good polarization purity over both frequency bands. According to [3], the bandwidth capability of the upper band is restricted. That is why the corrugation depth is set to  $3\lambda/4$  around 118.75 GHz (1.89 mm). As a consequence, this depth is  $\lambda/4$  at 40 GHz. It is expected that the bandwidth of the lower band is large enough to include the 52.5 GHz frequency band. To get a low return loss, the corrugation depth linearly decreases from  $\lambda/2$  to  $\lambda/4$  in the transition between the smooth walled input waveguide and corrugated horn as described in [3]. In the upper band, the corrugation depth should decrease from  $\lambda$  to  $3\lambda/4$ . Once again, the design is based on the critical upper band and the depth of the first corrugation is set to  $\lambda$  at 118.75 GHz (2.53 mm). This depth corresponds to  $\lambda/2$  at 60 GHz, which is near from 52.5 GHz. In addition, the width of the corrugation may also increase linearly in the transition zone in order to improve the bandwidth, like for example in [4].

These design rules and some optimization by trial and error led to the design presented on figure 2. A hyperbolic profile was chosen for a smooth transition in the throat region. Figure 2 also presents the performances of this horn. They are

evaluated with the IEROS software based on the Method of Moment (MoM) for rotationally symmetric structures [5]. The major drawback of this first design is the size of the first corrugations. For example, the first slot is very thin and deep : depth = 2.53 mm, width = 0.21 mm. The ratio depth/width is 12, while the manufacturing constraints (not communicated at this stage of the study) require a ratio below 7 for such small dimensions.

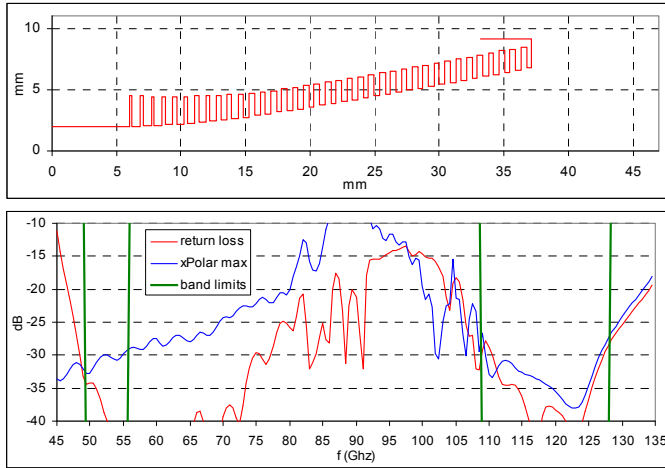


Fig. 2 Inner profile, return loss and peak cross polarization of the dual band single depth corrugated horn designed by trial and error.

### B. Optimization

Despite of these drawbacks, this design is a good starting point for an automated optimization. In order to limit the number of variables, the horn is conical (defined with a variable flare angle) and the corrugation geometry (pitch, width and depth, as defined in [3] for example) is variable but is the same for every tooth in that conical part. In that study the hyperbolic profile provides good results and a hyperbolic profile quickly join a conical profile after the throat region. In addition, a conical horn is easier to manufacture by classical milling. The total number of teeth is fixed and limited to reduce the CPU time : 37. The number of teeth in the mode converter is also fixed : 9. Each tooth in that part is defined with 4 variables parameters (pitch, width, depth, and position). A total of 40 variables is reached. The limits of these variables are mainly determined by the manufacturing constraints.

Various optimizers were tried, mainly gradient-based algorithms. Even if the optimization is automated, some trial and error was needed to choose the algorithm, the weighting coefficient for the return loss and the cross polarization, the number of frequency points,... The result of the optimization is presented in figure 3.

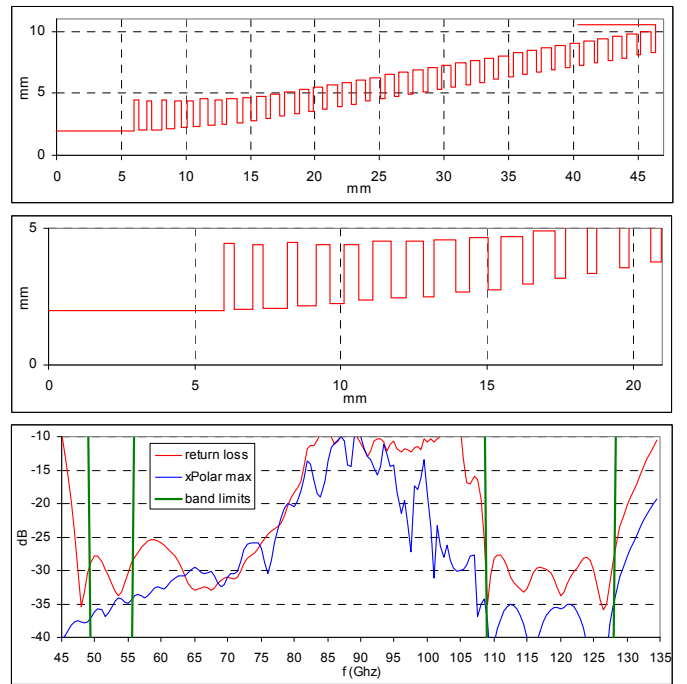


Fig. 3 Inner profile of the optimized corrugated horn. The middle part shows a zoom on the throat region. The return loss and the peak cross polarization are computed from 45 GHz to 135 GHz.

## III. FOOTPRINT OVERLAP

### A. Long horn

The return loss and the cross polarization were minimized for a short horn. As said in the introduction, the radiation pattern of the entire antenna (horn + reflector) is computed for a longer version : same throat region, same output corrugations, same flare angle, but higher number of teeth. Figure 4 presents this horn. It is checked that the return loss is mainly determined by the throat region. The cross polarization is slightly different for the long horn, but this difference is negligible for the present application.

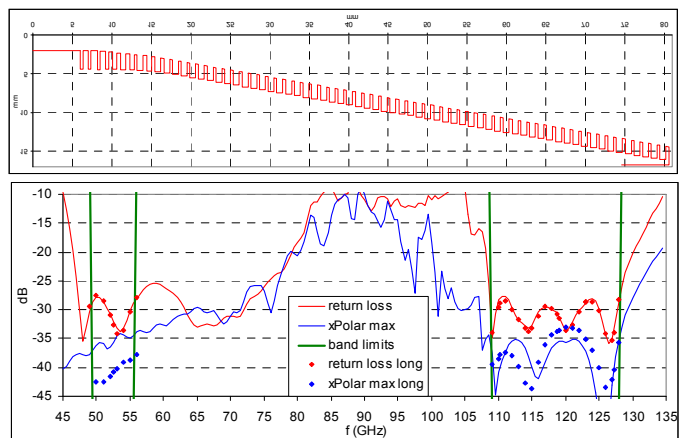


Fig. 4 Inner profile of the long horn, deduced from the horn optimized in the previous part and prolonged. The return loss and the peak cross polarization

are compared with the results of the shorter version in the operating frequency bands.

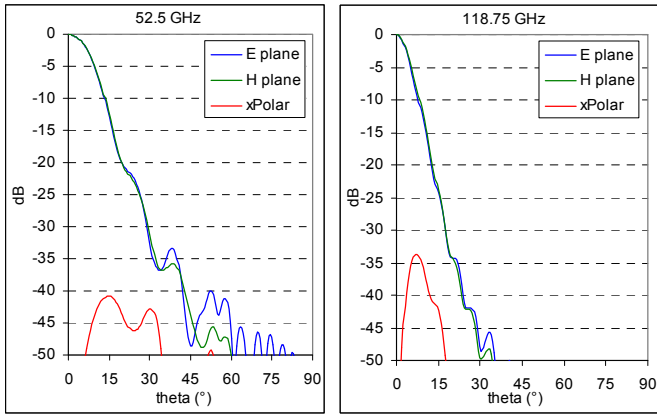


Fig. 5 Far field radiation patterns of the feed shown in figure 4. The center frequencies are considered.

The reflector antenna is simulated with a Physical Optics (PO) software developed by IEEA [6]. The reflector is represented with a 3D triangular mesh. The far-field patterns of the feed are presented in figure 5. They are used to illuminate the reflector. The PO currents are evaluated on every triangle. These currents are integrated to compute the radiation pattern of the entire reflector antenna. In the latest version of the software, this integration is performed by the graphics processing unit (GPU) and not the classical graphics processing unit (CPU). The observed speed up is between 5 and 10 times (Geforce 8600GT vs. Athlon 64 4000+), depending on the number of triangles and directions of observation. Figure 6 shows the simulated offset reflector.

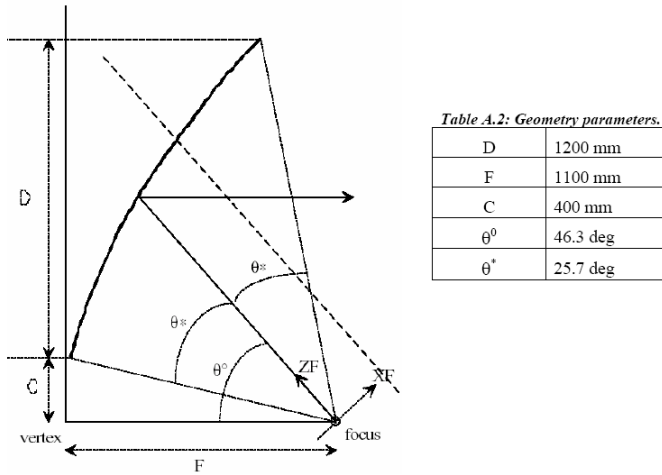


Fig. 6 Cross section of the offset parabolic reflector

The far field pattern of the entire reflector antenna is used to compute the  $-3$  dB footprint at the center frequencies (52.5 GHz and 118.75 GHz). As mentioned in the introduction, these footprints are to be identical to test the same point of the atmosphere. This is estimated by the footprints overlap :

ratio of the footprints intersection area and the biggest footprint area. The obtained result is presented in figure 7. The computed overlap is 89.4 %. This result is very near the requirement of 90 %. However, a higher overlap would be preferable to have some margins, in case of manufacturing errors.

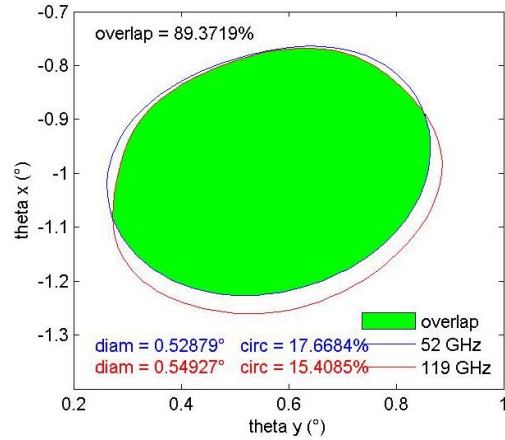


Fig. 7  $-3$  dB footprints at center frequencies and the corresponding overlap. The spherical coordinates are named (theta x, theta y) instead of (theta, phi) in this figure.

### B. Horn position

Until now, the initial aperture position was considered. Several horns are used with the same reflector. As a consequence, the initial position of the feed presented in this work is defocused. The position is presented in the upper part of figure 8. If the feed is located at the focus point of the reflector, an excellent footprint overlap is observed. The figure 8 shows the degradation of the overlap as the feed is moved in the focus plane. This result is useful to determine a position compliant with the overlap requirement and the mechanical constraints.

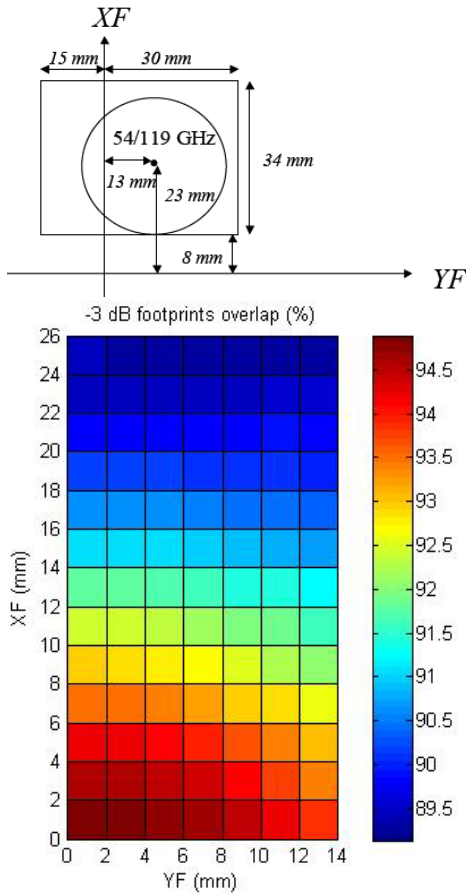


Fig. 8 -3 dB footprints overlap as a function of the feed position in the focal plane. The upper part of the figure defines the (XF,YF) coordinates. It also shows the initial position of the feed.

### C. Horn profile

The advantage of the previous solution is that the feed is unchanged. However, it needs to reorganize the positions of the other horns in the focal plane. In this part, another solution is investigated. In the introduction, it is supposed that the return loss and the cross polarization is mainly determined by the throat region and by the corrugations geometry. There is a remaining degree of freedom : the profile of the horn. In a certain extent, this last parameter can modify the radiation pattern without affecting the return loss and the cross polarization. In the case under study here, a spline curve is used to replace the conical profile of the horn. The control points of this spline curve are the variables of a new automated optimisation process. The result of the optimisation is presented in figure 9. A slight modification of the horn profile can improve the -3 dB footprints overlap. However, a conical profile is easier to manufacture by classical milling.

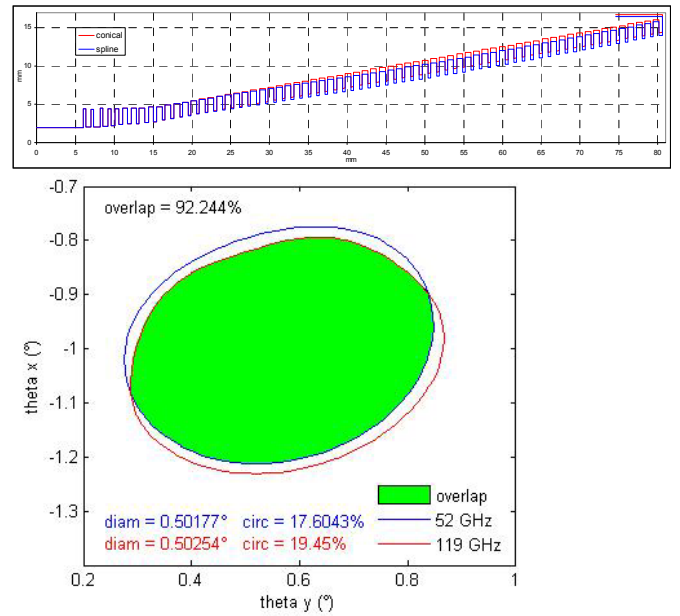


Fig. 9 Optimized spline profiled corrugated horn (blue) compared with its conical counterpart (red). Computed -3 dB footprints for 52.5 GHz and 118.75 GHz with this feed at the initial position.

## IV. CONCLUSIONS

Almost all the requirements are reached with the proposed single depth corrugated horn. The automated optimization plays an important role in the design of this horn. The -3 dB footprints overlap could be improved by moving the feed in the focal plane or by choosing a better horn profile. The first solution may affect the other feeds in the focal plane. The second is more difficult to manufacture.

## ACKNOWLEDGMENT

This R&D study is conducted by Astrium & IEEA under the ESA contract n° 20158/06/NL/JA.

## REFERENCES

- [1] L. Costes, N. Mohamed, J.-C. Orhac, J.-M. Goutoule, J.-P. Adam, Y. Béniguel, A. Berthon, M. Van der Vorst, "Multi-Frequency Feeds for Earth Observation Applications", proceedings of 30th ESA Antenna Workshop on Antennas for Earth Observation, Science, Telecommunication and Navigation Space Missions, Noordwijk, 2008.
- [2] Olver, *Microwave horns and feeds*, IEE electromagnetic waves series, Vol. 39
- [3] Christophe Granet and Graeme L. James, "Design of Corrugated Horns : a Primer", *IEEE Antennas and Propagation Magazine*, vol. 47, no. 2, pp. 76-84, April 2005.
- [4] Y. Béniguel, A. Berthon, C Van't Klooster, and L. Cost, "Design realization and measurements of a high performance wide-band corrugated band", *IEEE Transactions on Antennas and Propagation*, vol. 53, no. 11, pp. 3540-3546, November 2005.
- [5] A. Berthon, R. Bills, "Integral Equations Analysis of Radiating Structures of Revolution", *IEEE Transactions on Antennas and Propagation*, vol. 37, no. 2, pp. 159-170, February 1989.
- [6] IEEA website : [www.ieea.fr](http://www.ieea.fr)